An integrated approach for tracking climate-driven changes in treeline environments on different time scales in the Valle d'Aosta, Italian Alps

Version accepted for publication
Reuse is restricted to non-commercial and no derivative uses

The Holocene

1–14

DOI: 10.1177/09596836211025974

journals.sagepub.com/home/hol

An integrated approach for tracking climate-driven changes in treeline environments at different time scales in Valle d'Aosta, Italian Alps

Anna Masseroli[1], Giovanni Leonelli[2,3], Umberto Morra di Cella[4], Eric P. Verrecchia[5], David Sebag[5,6], Emanuele D. Pozzi[1], Valter Maggi[3,7], Manuela Pelfini[1], and Luca Trombino[1]

1 Department of Earth Sciences "A. Desio", Università degli Studi di Milano, Milano, Italy;
2 Department of Chemistry, Life Sciences and Environmental Sustainability, Università degli Studi di Parma, Parma, Italy;
3 Department of Earth and Environmental Sciences, Università degli Studi di Milano-Bicocca, Milano, Italy;
4 Environmental Protection Agency of Aosta Valley, ARPA Valle d'Aosta, Saint Christophe, Italy;
5 Institute of Earth Surface Dynamics, Faculty of Geosciences and the Environment, Université de Lausanne, Switzerland;
6 IFP Energie Nouvelles (IFPEN), Direction Géosciences, Rueil-Malmaison, France;
7 Istituto di Geoscienze e Georisorse, Consiglio Nazionale delle Ricerche, Pisa, Italy;

e-mail and ORCID:

anna.masseroli@unimi.it, http://orcid.org/0000-0002-9845-2608
giovanni.leonelli@unipr.it, http://orcid.org/0000-0002-1522-1581
u.morradicella@arpa.vda.it,
eric.verrecchia@unil.ch, http://orcid.org/0000-0001-7105-256X
david.sebag@ifpen.fr, http://orcid.org/0000-0002-6446-6921
lele.pozzi@live.it,
valter.maggi@unimib.it, http://orcid.org/0000-0001-6287-1213
manuela.pelfini@unimi.it, http://orcid.org/0000-0002-3258-1511
luca.trombino@unimi.it, https://orcid.org/0000-0002-7714-2686

Abstract

Both biotic and abiotic components, characterizing the mountain treeline ecotone, respond differently to climate variations. This study aims at reconstructing climate-driven changes by analyzing soil evolution in the late Holocene and by assessing the climatic trends for the last centuries and years in a key high-altitude climatic

treeline (2515 m a.s.l.) on the SW slope of the Becca di Viou mountain (Aosta Valley Region, Italy). This approach is based on soil science and dendrochronological techniques, together with daily air/soil temperature monitoring of four recent growing seasons. Direct measurements show that the ongoing soil temperatures during the growing season, at the treeline and above, are higher than the predicted reference values for the Alpine treeline. Thus, they do not represent a limiting factor for tree establishment and growth, including at the highest altitudes of the potential treeline (2625 m a.s.l.). Dendrochronological evidences show a marked sensitivity of tree-ring growth to early-summer temperatures. During the recent 10-yr period 2006-2015, trees at around 2300 m a.s.l. have grown at a rate that is approximately 1.9 times higher than during the 10-yr period 1810-1819, one of the coolest periods of the Little Ice Age. On the other hand, soils show only an incipient response to the ongoing climate warming, likely because of its resilience regarding the changeable environmental conditions and the different factors influencing the soil development. The rising air temperature, and the consequent treeline upward shift, could be the cause of a shift from Regosol to soil with more marked Umbric characteristics, but only for soil profiles located on the N facing slopes. Overall, the results of this integrated approach permitted a quantification of the different responses in abiotic and biotic components through time, emphasizing the influence of local station conditions in responding to the past and ongoing climate change.

Keywords

Geopedology, soil temperature, dendrochronology, treeline ecotone, climate change, western Italian Alps, late Holocene

Introduction

Treeline ecotones, defined as the transition belt in mountain vegetation from closed forest to treeless alpine terrain (Körner, 1999), are one of the most distinctive features in the Alpine landscape and are useful for studying the velocity of landscape dynamics in relationship to climatic changes. Since the ecological dynamics of the alpine treeline ecotone is mainly driven by climate, the treeline is widely considered as a climatic boundary. Indeed, several climatic parameters influence the maximum altitude of the treeline, such as wind, duration of snow cover, frequency and intensity of precipitation, as well as temperature (e.g. Holtmeier and Broll, 2005). Among these parameters, air and soil temperatures are the most important because they impose physiological limits to tree growth. Gehrig-Fasel et al. (2008) suggested that the value of seasonal mean soil temperature can be the most robust indicator for the position of the treeline and calculated the root-zone temperature range at 7 ± 0.4°C for treelines in the Swiss Alps, not far from the root-zone temperature of 6.7 ± 0.8°C modeled by Körner and Paulsen (2004) to estimate the treeline position at the global scale.

Typically, at the site scale, the response time to specific climatic inputs may vary both in biotic and abiotic components, greatly increasing also the possible interactions in the treeline ecosystem. Treelines are related to climate conditions (e.g. Beckage et al., 2008; Burga, 1991; Hughes et al., 2009; Kullman, 2001; Kullman and Öberg, 2009; Leonelli et al., 2011; Scapozza et al., 2010; Vittoz et al., 2008), but their upward shift may be a rather slow process, also under ameliorating climatic conditions, and takes place following fragmented patterns within a region, mainly because of the presence of active geomorphological processes or because of topographic constraints close to the ridges (e.g. Butler et al., 2009; 2003; Leonelli et al., 2016; Macias-Fauria and Johnson, 2013; Masseroli et al., 2016; Virtanen et al., 2010). Actually, the modern treeline altitude at some sites in the European Alps may still be some hundred meters below the historical treelines (e.g. Nicolussi et al., 2005), underlining that the upward recolonization of high-altitude belts may take times up to decades and centuries. On the contrary, under cooling conditions, all trees above a certain altitude may die from one year to the other, causing an immediate downward shift of the treeline.

Almost immediate responses to climate are also recorded in the tree-ring chronologies of trees growing at the treeline belt, whose growth is strongly limited by climate. Indeed, trees are able to record long series of environmental information with annual resolution in the tree rings, thus acting as natural archives of climate variability through centuries and millennia (Hughes, 2002). Tree-ring chronologies from the temperature-limited environments of the Alps are widely used for reconstructing past climate parameters for periods prior to instrumental data as well as for analyzing the effect of recent global warming on tree-ring growth (e.g. Büntgen et al. 2005, 2011; Coppola et al. 2012, 2013; Corona et al. 2010). Tree-rings may therefore be considered as a useful tool for studying the temporal dynamics of climate at local and regional scales, with annual resolution taking also into account disturbance factors. Moreover, analysis and dating of tree rings from buried logs located above the treeline allow tree growth rates and trends to be compared in different time periods, as well as the reconstruction of previous environmental conditions including the past timberline position (e.g. Nicolussi et al., 2009; Pelfini et al., 2014).

Although, soil responses to changing climate are a long-term process (Holtmeier and Broll, 2018), the ongoing climatic change, and the consequent altitudinal upward shift of the vegetation belts in mountain areas, may induce the shift of the linked soil processes (e.g. brunification, podzolisation, cryoturbation; Chersich et al., 2015) with century-long response times. For example, the podzolisation line, which is partly related to acidification by the coniferous tree litter, may advance to higher altitude due to the upward shift of the timberline, the boundary of the podzolisation domain. The ongoing climate change, affecting soil temperature, moisture, and snow cover, may influence soil weathering and carbon and mineral balance (Dawes et al., 2017; Egli and Poulenard, 2016; Freppaz and Williams, 2015; Hagedorn et al., 2010), causing a modification of soil properties (e.g. water supply, decomposition, and plant-available nutrient supply) that may affect vegetation growth and colonization (Holtmeier and Broll, 2007; Müller et al., 2016; Sullivan et al., 2015). In turn, tree

vegetation itself influences pedogenesis and thus, soil nutrient conditions, by amount, coverage, and quality of litter (Holtmeier and Broll, 2007; Phillips and Marion, 2004). However, the mosaic of soil types that characterizes the treeline ecotone is also closely related to the varying conditions of the local topography. Pronounced dissimilarities exist between soils developed at sites with variable topographic conditions (e.g. exposure, relief forms and gradients; Egli et al., 2010; Holtmeier and Broll, 2018; Masseroli et al., 2020), thus influencing the soil response to climate change. Despite there are no treeline-specific soil types in the temperate mountains (Holtmeier and Broll, 2018), the study of soil properties and characteristics proved to be a useful tool for the investigation and reconstruction of the response of sensitive environments to the past and ongoing climate changes (D'Amico et al., 2016, 2019), as they are the results of the interactions between different environmental factors (i.e. climate, organic activities, relief, parent material, and time; Jenny, 1941).

In order to assess the past and ongoing environmental evolution at different time-scales in a key high-altitude climatic treeline, we analyzed air/soil temperature data collected over four years of observations (daily scale, present conditions), tree-ring growth (secular scale), and soils (for collecting long-term environmental information) at the Becca di Viou mountain in the Aosta Valley Region (western Italian Alps). Since the climatic treelines in high mountains are highly sensitive to climate and environmental changes, the main aim of this research is to reconstruct the past environmental changes that occurred through time at the Becca di Viou study site, in order to better understand the biotic and abiotic responses to the climatic inputs through time, compared to the more recent climate conditions.

Study area

The study area presents one of the highest treelines in the Aosta Valley region and is characterized by extensive mass wasting deposits and patchy stabilized Alpine grassland (Figure 1a, b). This latter is more widespread in the west oriented slope portion, probably due to the presence of a barn and an alpine pasture, where cows graze during summertime, located about 200 m below the forest-treeline boundary (at 2080 m a.s.l.). In the upper portion of the area, from 2700 m a.s.l. and above, the site is characterized by rock faces covering more than 90% of the total surface. At lower altitudes, active talus slopes and rockfall deposits characterize the whole treeline belt down to 2300 m, covering up to approximately 40% of the total surface with unconsolidated debris (Leonelli et al., 2011). The low activity of geomorphic processes allows soil formation and colonization of herbaceous and tree vegetation where consolidated deposits are present, resulting in the establishment of continuous open forests of European larch (*Larix decidua* Mill.) in the lower portion of the area and of sparse trees towards the highest altitudes.

The Becca di Viou study site is located in the Austroalpine geological domain. In the study area, the Mont Mary unit emerges. In this area, an undifferentiated polymetamorphic complex (MMY), mainly composed of paragneiss with relic texture and assemblages of pre-Alpine age and locally displaying mylonitic textures,

146 metapegmatites (MMYb), and paraschists alternating with gneissic pegmatite (MMYc; Dal Piaz et al., 2010),
147 outcrop.
148
149 In the study area, a low degree of development characterizes the soils, which are mainly Leptosol, and in some
150 cases, with a surface layer rich in humus (Umbrisol) including a lot of coarse fractions, a typical feature of
151 high mountain areas. In the lower altitude slope portion, soils are also of Regosol type (Carta Ecopedologica
152 d'Italia 1:250000, Geoportale Nazionale, 2013,
153 http://wms.pcn.minambiente.it/ogc?map=/ms_ogc/WMS_v1.3/Vettoriali/Carta_ecopedologica.map).
154
155 The climate in the region has a semi-continental temperature regime (Dfb climate type following the Köppen-
156 Geiger classification (Peel et al. 2007)). According to the meteorological records in the valley bottom close to
157 the study site (at the Saint Christophe meteorological station (545 m a.s.l.); ARPA Valle d'Aosta) and during
158 the period 1995-2012, the temperature data display a winter minimum in January (-0.4°C) and a summer
159 maximum in July (21.7°C), with an annual variation in temperature slightly over 22°C. Regarding rainfalls,
160 they are scarce in the main valley (approximately 680 mm) but more abundant at the high altitudes of the
161 treeline (1000–1200 mm; Mercalli et al., 2003), mainly occurring during summer months.
162
163 Concerning the vegetation of the study area, Norway Spruce (*Picea abies* (L.) H. Karst) and Scot Pine (*Pinus*
164 *sylvestris* L.) forests dominate the belt under 1900 m a.s.l., whereas the closed mixed forest, dominated by
165 European Larch and Swiss stone pine (*Pinus cembra* L.), reaches higher altitude (about 2300 m a.s.l.;
166 Forestazione-foreste di protezione, Geoportale Valle d'Aosta, 2013,
167 http://geonavsct.partout.it/pub/GeoForeste/index.html?funzione=GF_PROTE). Above the timberline, the area
168 is characterized by a semi-natural treeline ecotone, mainly composed of European larch. In 2008, the treeline
169 was located at an average altitude of 2515 m a.s.l, while the species line of the European larch was found at
170 2545 m a.s.l. in 2009 (Leonelli et al., 2011; Figure 1b). However, up to high altitudes, there are several sparse
171 portions of alpine grassland and shrubs.
172
173 **Material and Methods**
174 *Monitoring of air and soil temperatures*
175 From October 2008 to October 2012, air and soil temperatures were monitored at the treeline belt (Lower
176 Treeline; at 2345 m a.s.l.) and in the area above. Only the soil temperature was monitored at higher altitudes,
177 i.e. at the tree species line (SL; two datalogger at 2545 m a.s.l.) and at the potential treeline (PT30; 2625 m
178 a.s.l.), whose altitude was estimated by considering the occurrence of > 100 days with an air temperature above
179 5°C along a 30-yr period (1975–2004; Leonelli et al., 2011). The five dataloggers of ARPA Valle d'Aosta
180 (HOBO Pro Series; ONSET 1998) recorded air and soil temperatures every 10 to 30 minutes: the recording
181 rate was set according to the datalogger memory capacity. The air temperature datalogger was protected by a

sun shield, whereas the soil dataloggers were included in stagnant boxes and the sensors put at 10 cm-deep from the ground surface. Although some technical problems arose during the monitoring period (low battery levels, cable disruption, malfunctioning), high-resolution soil and air temperature changes were obtained for each of the four growing seasons from 2009 up to 2012. These data were used for characterizing soil temperature conditions in the upper portion of the soils of the study area, and for comparing the current temperature conditions at the study site with references to treeline temperature found in the literature.

Tree-ring chronology construction from time series

Twenty-four old, living, and standing trees of European larch were sampled in the open-forest belt between 2250 and 2350 m a.s.l., by taking two cores per trees using a Pressler's increment borer. Samples were prepared with standard techniques gluing the cores on wood supports and preparing transversal surfaces by means of a plane sanding machine. Tree-rings widths were measured on each core by means of a LINTAB connected to a computer, using the TSAP-Win software (RINNTECH, Heidelberg, Germany): overall, 48 raw individual growth series were obtained. Each growth series was visually and statistically cross-dated with the other growth series from the same tree and with the growth series from the other trees, thus eliminating any potential dating error. A growth series was eliminated because of anomalous growth patterns with respect to the other series. The COFECHA program was used for the statistical cross-dating within and between trees, whereas, the RCSsigFree_v.45 program was run for the construction of a "signal-free" chronology (Melvin and Briffa, 2008; both software, www.ldeo.columbia.edu). We adopted the signal-free RCS standardization approach and applied age-dependent spline smoothing (with initial stiffness of 50 yr) for detrending the individual series (Melvin and Briffa, 2014). The signal-free RCS approach mitigates the potential "end effect" bias found in the simple RCS due to the potential conservation of the 20th century growth-increase signal when calculating the regional curve based only on living trees.

Detection of the climate signal

The detection of the climate signal recorded in the site chronology was performed using a correlation function approach. The site chronology was analyzed against monthly and seasonal values of temperature for the grid cell 45.75 N, 7.25 E comprising the study area (CRU TS Version: 4.01, Harris et al., 2014). Monthly variables from June of the year previous to growth up to September of the year of growth were selected together with aggregate variables of August-to-October (ASO-1) of the year previous to growth and June-to-August (JJA) of the year of growth. Moreover, a linear regression analysis of the standard chronology on summer (JJA) temperature was performed in order to investigate the spread of the points along the regression line and the signal strength. The same correlation analysis was performed also using precipitation variables (not shown).

Soil sampling

Seven soil profiles were described, according to Jahn et al. (2006), and sampled slightly below the current treeline at an altitude ranging from 2100 m a.s.l. to 2400 m a.s.l. (Table 1). An altitudinal transect of three soil profiles (BV16/01, BV16/02 and BV16/03), ranging from 2300 m a.s.l. to 2400 m a.s.l., was located on the right portion of SW slope of Becca di Viou, while another altitudinal transect of three soil profiles (BV16/04, BV16/05 and BV16/06), ranging from 2325 to 2370, was placed on the left portion of SW slope of Becca di Viou (Figure 2). As a comparison, one soil profile (BV16/07), located at 2110 m a.s.l., was excavated in a forested area (Figure 1b; Table 1). For each soil profile, coordinates were recorded using a GPS device and from each identified soil horizon, between 0.5 to 2 kg of material were sampled for laboratory analyses (Avery and Bascomb, 1982; Cremaschi and Rodolfi, 1991; Gale and Hoare, 1991).

Soil mineral matrix analysis

Soil pH was estimated on fine earth using a soil solution ratio of 1:2.5 (soil: distilled water). Particle size distributions were determined after sample pretreatment with H_2O_2 (130 volumes) using a combined method consisting of sieving for particles between 2000 μm and 63 μm, and aerometry (Casagrande aerometer method) for the finer particles (< 63 μm).

Acid ammonium oxalate and dithionite-citrate-bicarbonate were used to extract iron and aluminum from amorphous oxides and hydroxides ("active" forms, Fe_o and Al_o), and iron and aluminum form non-silicate forms ("free" iron, Fe_d and Al_d), respectively (Ministero delle Risorse Agricole Alimentari e Forestali, 1994). The amount of solubilized iron and aluminum in the supernatant was determined by means of a 4100 MP-AES (Agilent) after the appropriate dilutions. Since no data have a %RSD (Relative Standard Deviation) of concentration > 3.5 and/or a not detectable clear peak, all results were considered valid, whereas the data close to the detection limit of the instrument were approximated to the minor concentration detectable (< n in Table 2). In addition, both the iron activity index (Fe_o/Fe_d) and the illuviation (podzolization) index ($Al_o+½Fe_o$) were calculated (IUSS Working Group WRB, 2015); the amount of crystalline iron oxides (Fe_{cry}) was calculated by the difference between the dithionite- and the oxalate-extractable Fe ($Fe_{cry}= Fe_d-Fe_o$; Bascomb, 1968; Cremaschi and Rodolfi, 1991; Zanelli et al., 2007).

Soil organic matter analysis

Total organic C (C org.) and N (TN) contents were determined using the Walkley-Black (Walkley and Black, 1934) and Kjeldahl methods (Kjeldahl, 1883), respectively. The OM properties were obtained by thermal analysis performed with a Rock-Eval® 6 pyrolyser (Vinci Technologies, France). About 60 mg of crushed material, previously sieved (< 2 mm), were analyzed for each horizon. Standard parameters – Total Organic Carbon (TOC), Hydrogen Index (HI) and Oxygen Index (OI) – were calculated according to the conventional procedure (Behar et al., 2001; Lafargue et al., 1998). In addition, two thermal parameters related to the most reactive fraction of soil OM (i.e. pyrolyzed carbon) were computed according to Sebag et al. (2016). By construction, the R-index relates to the thermally resistant and refractory pools of soil OM, while the I-index

is related to the ratio between the thermally labile and resistant pools (see Sebag et al., 2016 for details). As derived from a mathematical construct, these two indexes may be inversely correlated along a constant line ("*humic trend*" in Sebag et al. 2016; *"decomposition line"* in present study) when OM stabilization results from progressive decomposition of organic components according to their biogeochemical stability. Then, a decrease in labile pools result in a concomitant increase in more thermally stable pools, as observed in compost samples and undisturbed soil profiles (Albrecht et al., 2015; Matteodo et al., 2018; Schomburg et al., 2018, 2019; Sebag et al., 2016). Matteodo's dataset composed of 46 soil profiles selected across various eco-units in Swiss Alps (Matteodo et al., 2018) was used for comparison. Finally, the stable carbon and nitrogen isotope abundances in the samples were determined using a Thermo Scientific Delta V device. The $\delta^{13}C$ and $\delta^{15}N$ values are reported relative to the Vienna Pee Dee Belemnite standard (VPDB) and air-N_2, respectively. Laboratory standards were calibrated relative to international standards.

Results

Air and soil temperature results

The monitoring of air temperatures at the study site gave ranges between approximately -15 °C (for January 2010 and 2011 and for February 2012) and 17 °C (usually reached in August; Figure 2) during the recent period. Soil temperatures, instead, showed markedly higher minimum temperatures, close to 0 °C during winter for all dataloggers, except for the *Ts Species line 2*, which reached approximately -3 – -4 °C. As regards maximum soil temperatures, some dataloggers recorded values higher than air temperatures: the datalogger *Ts potential treeline 30 yr* usually overpassed the temperature of 20 °C in August; the *Ts species line* reached 19.9 °C, whereas the other dataloggers reached approximately 17 °C (Figure 2). For what concerns the average soil temperature during the growing season, values slightly exceeded 11 – 12 °C, except for *Ts Species Line 2* that recorded lower temperature values at approximately 8.5 – 9.5 °C. The growing season lengths (Körner and Paulsen, 2004) have only been evaluated for the complete periods of 2009, 2011, and 2012, and resulted in 166 ± 15 days.

Temperature and precipitation variations by the grid cell 45.75 N – 7.25 E over the common period 1902-2015 (Fig. 3; CRU TS Version: 4.01, Harris et al., 2014) display a visible increasing trend for both variables. The mean JJA temperature is 8.8°C ± 1 °C and shows a local maximum in the 1940s and a recent increasing trend in temperature since the late 1970s. According to the linear trend calculated over 1902-2015, this temperature variable exhibits an increasing rate of +1.6°C in 100 yr. Precipitation of the water year (October of the previous year to September) is 1827±258 mm in average, with maxima reached during summer (JJA; 524 mm) and minima during winter (DFJ; 403 mm). According to the linear trend calculated over 1902-2015, the October-to-September precipitations (i.e. a water year) have an increasing rate of +64.7 mm in 100 yr. By analyzing the seasonalized variables (not shown), this trend is mainly due to an increase in winter precipitations (DJF;

+38.6 mm) and summer precipitations (JJA; +16.0 mm), whereas spring precipitations show a decreasing trend (MAM; -5.9 mm).

Tree-ring chronology

The Becca di Viou tree-ring chronology spans over 204 years from 1812 to 2015 and it holds a good signal stability underlined by the EPS index value, i.e. EPS > 0.85 (Briffa and Jones, 1990) since 1852 (Figure 3). Slightly lower values of EPS > 0.76 are reached since 1823. The chronology showed periods of reduced tree-ring growth during the 1810-1820 period, the first years of the 1880s, the 1905-1915 and 1975-1980 periods. Although discontinuous, the recent positive trend of markedly higher tree-ring growth rates started during the 1980s, with the last 10-yr period presenting an average growth index value of approximately 1.9 times the growth index during the 10-yr period of minimum growth in the chronological record (i.e. 1810-1819). According to the linear trends calculated on z-scores over the 1902-2015 period, the tree-ring index has an increasing rate that is comparable, and higher, to that of the temperature record (+1.65 and +1.56, respectively, over 100 yr) (Table in Fig. 3).

An expected dependence of growth patterns during summer months is observed when comparing the temperature record with the associated dendrochronological data (Figure 4a). Temperatures of the late summer and early autumn, (August-to-October), mainly influence tree-ring growth in the following growing season. By analyzing seasonal variables aggregating couples of months, the dendrochronology data show correlations up to $r = 0.67$ ($p < 0.001$) with JJA and 0.49 ($p < 0.001$) with ASO-1. For precipitation, we found a statistically significant correlation, $r = -0.29$ ($p < 0.01$) only with June precipitation.

The regression of the ring-width index on the JJA variable, shows a clear dependence of tree-ring growth on the summer temperatures, with this climate variable explaining up to 45% of the tree-ring growth variability (Figure 4b). Therefore, the tree-ring growth patterns recorded in the dendrochronological data well follow the summer (JJA) temperature variability through time.

Soil matrix analysis

The studied soil profiles assume variable thicknesses (usually 30 to 60 cm) depending on the altitude range, vegetation cover, and geomorphological settings. The maximum thickness is found in soils that evolved under forest vegetation and the minimum thickness in soils developed at the treeline ecotone, with the exception of profile BV16/02, which is rather deep (75 cm), even if located at the treeline ecotone. Horizon colors show a clear uniformity in the area, particularly in regards to the hue values, which are never different from 10 YR or 2.5 Y. Soil structure is moderately expressed and it is mainly characterized by granular aggregates, or less frequently by subangular blocky aggregates (Supplemental Material Table S1).

Analyses of particle size distributions (PSD) carried out on soil profiles showed a marked presence of coarse material. The gravel fraction varied between 3.0% and 65.1%. Among the fine earth, the most representative particle size fraction is silt, which ranges from 15.0% to 62.4% of total weight (Figure 5), whereas the amounts of sand and clay, between 8.0 and 32.9%, and between 0.2 and 15.8%, respectively. All the analyzed soil profiles showed a decrease of the coarse component from bottom to top (Figure 5; Supplemental Material Table S2).

Like in all analyzed profiles, the BV16/02 profile displays a coarse fraction content increasing with depth, as well as a progressive decreasing trend in clay. However, its cumulative PSD curves (Supplemental Material Figure F1) show two distinct families of grain populations: one includes the superficial horizons (O and AC) and another the deeper horizons (2AB, 2Bw and 2BC). Moreover, the presence of a small stone line in the field, characterized by elongated subangular decimetric clasts, was observed between the AC and 2AB horizons.

All soil horizons' pH_{H2O} values range from 4.6 to 5.6 (Figure 5). Almost all measured pH vary by only a < 0.5 pH unit along the profiles.

Among the different forms of extractable iron, the free iron oxides (Fe_d) are the most common in the analyzed horizons: the total contents of free iron oxides (Fe_d) range from 3.23 to 19.03 g/Kg. However, the values of amorphous iron oxides (Fe_o) are slightly lower, ranging between <0.9 and 13.64 g/Kg. For both forms of extractable iron, particularly high values are observed in BV16/02 2AB and BV16/03 BC horizons (Table 2). On the contrary, the different forms of extractable aluminum, i.e. free aluminum oxides (Al_d) and amorphous aluminum oxides (Al_o), reached values between 0.99 and 5.82 g/Kg and between 0.63 and 6.01 g/Kg, respectively. The crystalline iron oxides Fe_{cry} content was very variable: in profile BV16/01, Fe_{cry} contents are low (1.65-3.3 g/Kg), whereas in profiles BV16/04 and BV16/05 the Fe_{cry} reached higher values, with a peak at 10.19 g/Kg in the BV16/04 AC horizon. The comparison between Fe_{cry} and Fe_o trends (Figure 6) underlines the presence of a trend between these two forms of iron in the more developed profiles. Moreover, a Fe_o peak in the B horizons is also clear. High values for the iron activity ratio (Fe_o/Fe_d) are found in the BV16/02 2AB (0.72), BV16/03 BC (0.86) and BV16/07 BC2 (0.68) horizons, whereas in the other horizons the iron activity index ranged from about 0.2 to 0.5 (Table 2). Finally, the results of the podzolisation index $Al_o + ½ Fe_o$ meet the conditions of podzolisation processes in the BV16/02, BV16/03 and BV16/07 profiles (IUSS Working Group WRB, 2015; Table 2).

Soil organic fraction analysis

Regarding the Total Organic Carbon (C org.) and Total Nitrogen (TN) contents, soil profiles are characterized by decreasing C org. and TN contents with depth (Figure 5, Supplemental Material Table S2). In more details,

the absolute quantities of C org. are variable depending on the type of profile and its depth (Figure 5). As expected, the highest content of C org. is found in superficial horizons, where values range from 55.8 (BV16/03) to 135 g/kg (BV16/07). In the superficial horizons, the highest contents of TN are found in the BV16/01 O (10.2 g/Kg) and BV16/05 O (10.3 g/Kg). Finally, the C/N ratio have values ranging between 8.8 and 14.7 in the superficial horizons.

According to the Rock-Eval pyrolysis analysis (Figure 7), the HI vs OI diagram displays a clear distinction between the surficial O and A horizons (at the top left), characterized by high values of HI inherited from fresh biological inputs, and the deeper B and C ones (at the bottom right), characterized by high values of OI related to transformed pedogenic and petrogenic organic matter (Figure 7a). The horizons belonging to the buried soil (BV16/02) have the highest OI values. Moreover, the thermal stability of the organic matter increases with depth in the analyzed soil profiles: the TOC decreases from the topsoil to the subsoil mineral layers and the R index increases, particularly in the horizons belonging to the buried soil (BV16/02 2AB, 2Bw and 2BC; Figure 7b, c). Moreover, the buried horizons (BV16/02 2AB, 2Bw and 2BC), placed at the bottom right in the I/R diagram, are separated from the other horizons and, are not exactly located on the "*decomposition line*" (see Sebag et al., 2016) contrary to the other studied horizons (Figure 7b).

Furthermore, the $\delta^{15}N$ trend in the profile BV16/02 shows a peculiarity: while in all other profiles the $\delta^{15}N$ increases with depth (Figure 8b), a trend inversion is found in this profile in correspondence with the 2AB and following horizons (2Bw and 2BC). The $\delta^{13}C$ distribution shows a trend inversion, not only in the BV16/02 but also in the BV16/01, BV16/05 and BV16/07 profiles (Figure 8a). However, the BV16/02 is the only profile showing a marked trend inversion and a negative $\Delta\delta$ (isotopic enrichment for each profile with reference to the first horizon), along the profile for both $\delta^{13}C$ and $\delta^{15}N$ (Figure 8c, d).

Discussion

The multidisciplinary analysis carried out at the high-altitude climatic treeline environments of Becca di Viou mountain allows the environmental changes characterizing the area to be reconstructed through time. Moreover, the results show that the abiotic and biotic components at the treeline ecotone respond to the past and ongoing climate changes at different time scales, also according to local station conditions.

As in other Alpine sites, the ongoing climate change in the study area is principally observable in rising air temperatures. Temperatures display a visible increasing trend for the period 1902-2015. The mean JJA (growing season) temperatures particularly show a local maximum in the 1940s and a recent increasing trend since the late 1970s, exhibiting an increasing rate of +1.6°C in 100 yr. The JJA mean air temperatures increase (+1.6°C in 100 yr) over the 1902-2015 period was also observable and of comparable magnitude in the tree-ring chronology , which show higher values during the recent years, starting from the 1980s. Although

correlations computed over long time periods with aggregate temperature variables may underline climate-growth responses in high altitude sites, often, over shorter time periods and using monthly variables may reveal decreasing correlation values in recent years, especially with June temperature. Decreasing trends in correlation values for early summer temperature and increasing negative trends for early summer precipitation were in fact obtained, e.g., in some studies carried out on Swiss stone pine and European larch in the Alpine treeline ecotone (Leonelli et al., 2009; Coppola et al., 2012;). These trends may be related to the so called the "divergence problem" - DP (Büntgen et al., 2008), causing a lack of correlation with climatic variables. The DP is closely related to the 20th century temperature's increase and can be attributed to the growing season prolongation as well as to local and global issues (D'Arrigo et al., 2008), including pollution, drought stress, etc. Numerous studies have reported an extension of the growing season in Europe due to the recent temperature increase (Menzel and Fabian, 1999; Menzel et al., 2006; Sparks and Menzel, 2002; Walther et al., 2002).

Indeed, the prolonged growing season and the warmer temperature conditions during the growing season has likely caused an upward shift of the vegetation belts, and of the treeline at the study site (Leonelli et al., 2011). But our analysis of soil temperature showed that the treeline could potentially reach even higher altitude than the present-day position. Indeed, the average soil temperatures, recorded by all dataloggers (including the ones at the Species Line) during the growing season (Figure 2), are higher than the reference soil temperature of 7° C for the treelines in the Swiss Alps (Gehrig-Fasel et al., 2008). Moreover, when comparing our results for the growing-season soil temperatures at the treeline with those proposed by Körner and Paulsen (2004) for the "Cool temperate W. Alps", the soil temperatures at Becca di Viou reached higher mean values associated to a longer growing season.

Both the radial growth of trees and tree recruitment are influenced positively by the increasing of temperature and precipitation rates but the patterns and the time of their responses may be different (Wang et al., 2006). Treeline advance may depend upon the coincidence of favorable conditions over sufficient years to permit establishment, growth, and survival. Moreover, treeline dynamics are affected by site and microsite conditions (e.g. microclimate, topography, soil, geomorphological processes) that can mask or modify the impact of climate change. The shift of the vegetation belt caused by the rising of soil and air temperatures, as well as land abandonment, although expected (e.g. Gehrig-Fasel et al., 2007; Vittoz et al., 2008), was not always observed at treeline sites (e.g. Klasner and Fagre, 2002; Mazepa, 2005). Indeed, plant communities are often decoupled from the local climate dynamics, as plants may be influenced by several biotic and abiotic interactions (Malanson et al., 2019).

The soil response to climate change is even more complex. The analyzed soil profiles show a weak degree of development, likely due to the slope steepness and other disturbance factors, such as erosional/depositional

processes, distinctive of mountain environments (Bollati et al., 2019; Legros, 1992; Zanini et al., 2015). The incipient stage of soil development is supported by the preponderant presence of coarse material, typical of Alpine soils on substratum made of debris or moraine deposits (Egli et al., 2001). As in other Alpine contexts (D'Amico et al., 2015; 2009), the influence of parent material in the Becca di Viou study site on soil properties is stressed not only by the particle size distributions, but also by the pH of the soil material (Figure 5). The soil pH displays only little variations throughout the profiles, and the superficial horizons are not characterized by the expected increase in acidity; in this light, the parent material mainly influences soil acidity.

In addition, Rock-Eval signatures support the weak soil development (Figure 7). Indeed, the OM of the superficial horizons presents a composition (HI, OI) quite comparable to the OM biogenic rich layers, like litter or humus (Matteodo et al., 2018; Sebag et al., 2016). The positions of O horizons in the I/R diagram (separate from the litter) indicate that decomposition processes are active and intense. On the other hand, most of A and B horizons indicate that OM stabilization related to pedogenic processes (i.e. organo-mineral complexation and aggregation; Lehmann and Kleber, 2015) is rather moderate.

Moreover, spatial heterogeneity and diversity of soil forming factors (Jenny, 1941) influence soil evolution, conditioning the soil response to climate change. An increment of soil development is observable all along the soil toposequences: as in other Alpine soils (Merkli et al., 2009; Egli et al., 2008), the profiles located at higher altitudes are thinner and less developed compared to those at lower elevation. In addition to the vertical zonality, the studied soils showed different properties according to their slope characteristics (i.e. aspect, slope) and geomorphological contexts. The gentler slope, and the less presence of rockfall deposits of the N facing slope than on S facing slope, influenced and still influences the soil development and their characteristics. However, the two soil toposequences seem to be mainly influenced by their aspect. The different aspects of the two slopes affect the climatic parameters (e.g. soil temperature), and therefore soil processes. Among the studied profiles, only those located on the N facing slopes (BV16/01, BV16/02 and BV16/03) show a shift from Regosol to soil with more marked Umbric characteristics, developing a B horizon. These data agree with other studies carried out in the Alps (Egli et al., 2006, 2009, 2010) showing the effect of slope aspect on soil development and characteristics. Egli et al., (2010) found that climatic parameters (e.g. lower temperatures, lower evapotranspiration, higher humidity) of N facing slopes can lead to an accumulation of labile, weakly degraded organic matter, and consequently, to a higher production of soluble organic ligands that enhance the migration (eluviation) of Fe and Al compounds. The different degree of illuviation of amorphous material is testified by the presence in B horizons on N facing slopes of higher concentrations of Al_o and Fe_o compared to those on S facing slopes (Table 2), and by a greater difference of Al_o and Fe_o between the uppermost soil layer and the B horizon on the N facing slope (Egli et al., 2006, 2009). Moreover, Fe_o/Fe_d ratio values, which may indicate both iron illuviation and extreme weathering effects (Waroszeski et al., 2013; Zanelli et al., 2007), are higher in the B horizons of soils located at N facing slopes (Table 2). The values of the Al_o + ½ Fe_o index

obtained at profiles BV16/02 and BV16/03, as at profiles BV16/07, seem to indicate a weak evidence, only partially recognizable in the field, of some podzolisation processes (Do Nascimento et al., 2008; IUSS Working Group WRB, 2015; Waroszewski et al., 2013; Table 2). The presence of a weak podzolisation (i.e. cryptopodzolisation) could promote the formation of Umbrisols (protospodic) (IUSS Working Group WRB, 2015). Anyway, the podzolisation index of profile BV16/02 is not easy to interpret, since the horizons (AC and 2AB) in which the index meet the condition of podzolisation processes belong to two different pedological units.

Some of the geopedological aspects mentioned above point out a soil weaker development than expected. This can be viewed as a consequence of unstable geomorphic conditions. On the other hand, this apparent disequilibrium can be explained considering soil as a highly resilient system capable of persisting over time and being able to absorb change and disturbance, still maintaining the same relationships between state variables (Holling, 1973). The studied profiles show a current shift between different pedogenetic processes (i.e. from Regosols to Umbrisols (protospodic)) induced by climate, but with a longer response time than vegetation. Therefore, the analyzed soils provide a realistic understanding of the systems behavior under the ongoing climate change.

The study of tree-ring growth and soil has also allowed us to collect information about the environmental changes that have occurred in the study area during the past. The high sensitivity of tree-ring growth to summer temperatures (JJA; Figure 4) allowed the growth trends in the chronology to be analyzed in order to reconstruct the past temperature variability, and underlined the presence of a recent positive trend. The site chronology emphasized periods of reduced and enhanced tree-ring growth at the study site. Indeed, in the last year of the chronology, i.e. in AD 2015, the growth index value reaches 2.3 times the growth over the 10-yr period of minimum growth in the chronology (1810-1819), i.e. during one of the Little Ice Age coolest periods (e.g. Lamb, 1995) in the area. Tree-ring growth in the last decade testifies the improved growing conditions for trees and confirms the high increase of air temperature conditions also at the treeline.

Whereas, the geopedological analyses allow the identification, in the profile BV16/02, of a past instability phase, interposed between two different stability phases and characterized by clearly developed soil units. A particle size discontinuity and a stone line between AC and 2AB horizons testified the presence of two different pedological (sedimentological) units (Figure 5): a buried unit, partially eroded and covered by debris deposits due to gravity processes, which was mainly induced by climatic oscillations or environmental changes (e.g. changes in vegetation cover), and a surficial unit, affected by present-day pedogenesis. The presence of a buried surface in BV16/02 is also highlighted by the results of stable isotopes: increases in $\delta^{15}N$ (Gerschlauer et al., 2019; Martinelli et al., 1999) and $\delta^{13}C$ with depth (i.e. in mineral horizons) are expected in soils under C3 vegetation (Balesdent et al., 1993). Whereas, in the BV16/02 profile, there is a marked inversion of both

$\delta^{15}N$ and $\delta^{13}C$ trends (Figure 8a, b). The $\delta^{15}N$ values show a trend inversion between AC and 2AB horizons, with first an isotopic enrichment and then a depletion. Other studies (e.g. Schatz et al., 2011) ascribe this variation to different soil organic matter mineralization due to different climatic conditions. In addition, the small $\delta^{13}C$ variations between superficial and buried units may reflect changes in soil organic matter mineralization (Zech et al., 2007). Moreover, some characteristics of soil organic matter support this interpretation. The Rock-Eval analysis revealed compositional indices (HI, OI) and thermal status (I/R diagram) specific of buried horizons (Figure 7a, b), with values typical of more decomposed and more stabilized organic matter (Sebag et al., 2016).

It is possible that $\delta^{15}N$ may be a more sensitive proxy than $\delta^{13}C$ in order to reconstruct environmental changes. Indeed, $\delta^{15}N$ is influenced by mineralization processes and especially by N losses, and this isotopic decrement most likely reflects a decrease of N losses due to the reduced SOM mineralization during the formation of the soil (Schatz et al., 2011). In terms of a paleoclimate, this can be attributed to lower temperatures and probably increased precipitations. Moreover, even if results of carbon stable isotopes suggest that C3 plants have been the main vegetation type for the entire time span during which the profile accumulated (the absence of C4 plants is typical of temperate and cold environments), the $\delta^{13}C$ variations remain interesting for the past climate reconstruction. Stevenson et al. (2005) have shown how the $\delta^{13}C$ gets lighter with increasing rainfall. Therefore, the presence in BV 16/02 of a buried unit characterized by a well-developed B horizon could be related to a past stable climate phase with different environmental and climate conditions interrupted by some changes. According to the stable isotope results, the buried soil can result from dynamics developed under more humid and colder climate conditions, which occurred after the LGM and Late-glacial period (formation period of the glacial deposits in the study area).

As evidenced from the obtained results, the soil and vegetation responses to climate change have been in the past, and are today, closely linked to various abiotic and biotic factors; these factors will probably influence the environmental response also in the future. Although the temperature data and dendroclimatological evidence underline a marked rise in temperatures in Becca di Viou area, the upward shift of the treeline was and will be likely halted in the next future because of specific geomorphological constraints (Leonelli et al., 2011). Nevertheless, an increase of tree density and an upward shift of the timberline could occur (Klasner and Fagre, 2002), promoting an advance to higher altitude of podsolization processes, which will be partly related to acidification by the coniferous tree litter. In the future, if the increasing temperature and precipitation rate conditions persist, the formation of Podzols (IUSS Working Group WRB, 2015) could happen. Indeed, higher precipitation rate leads to a higher amount of water percolating through the soil profile, thus promoting the migration of organic matter with Al-Fe complexes (Chersich et al., 2015). However, and considering the present day soil resilience, these soil processes shift towards podsolization will take place in an asynchronous time scale, respect to the establishment of the environmental conditions favorable to the podzolization itself.

In conclusion, this study underlines the importance of a multidisciplinary approach that, taking into consideration different natural archives, allows the study area evolution to be reconstructed in order to understand the complexity of the factors acting at high altitude environments.

Conclusions

As previous studies have demonstrated, the treeline at the Becca di Viou site has moved upward of approximately 75 m since 1950 (Leonelli et al., 2011); but further shifts towards higher altitudes are probably constrained by the slow evolution of soils, their scarcity, the topography, i.e. the steep slopes close to the ridges, as well as the presence of extensive gravity processes. Overall, based on a multi-proxy approach, this study emphasized the different response-times involving biotic and abiotic components in high-altitude treeline ecosystems undergoing the same climate inputs through time. As the soil temperature monitoring at the Becca di Viou site has proven, the ongoing temperature conditions at the treeline, and at the species line during the growing season, are already approximately 3°C above the modeled temperature limits of 7°C in the region. Thus, soil temperatures at the current elevations of the treeline, and the species line, do not represent anymore the main limiting factor either for tree establishment or growth at the highest altitudes.

Changes of climate conditions at the century scale are well recorded in the tree rings that document, with an annual resolution, the growing season temperature conditions, i.e. June and July. The ongoing trend in growth rates underline the exceptional period that high-altitude trees are facing nowadays at this site. In the recent 10-yr period (2006-2015), trees are growing at a rate that is approximately 1.9 times the growth during one of the coolest periods of the Little Ice Age (1810-1819), and 2.3 times for the last tree ring of 2015.

Tree rings proved to be a highly sensitive climate proxy with an annual resolution and a rapid response time, whereas treelines shift, and especially soils, showed slower dynamics, being also influenced by other environmental parameters. Soils show a resilience in relationship to the changeable environmental conditions: few variations of pedogenetic processes are in progress and a shift to higher altitude of podsolization processes is only partially visible in the soils located at N facing slope (Umbrisols protospodic).

Moreover, soil hold information about past environmental conditions, recording both the stability and instability phases. In BV16/02 profile, it is possible to reconstruct the succession of different phases of biostasy, during which the soil developed, and a phase of rhexistasy, during which the soil was eroded and finally buried, likely because of climate variations that occurred during the Holocene.

Acknowledgments

The Authors wish to thank the Regione Valle d'Aosta for the sampling permits, Saint-Cristophe and Roisan municipality for the vehicle transit permit, and Roberta Righini for the first assessment of the datalogger

temperatures. The authors are grateful to Dr. Compostella and Dr. Ferrari for their assistance in laboratory analyses. Rock-Eval® is a trademark registered by IFP Energies Nouvelles. The authors thank the International Relations from the University of Lausanne who provided travel funds between Italy and Switzerland. The authors also thank the staff at the University of Lausanne (Switzerland) for completing the Rock-Eval® analyses, and they are particularly grateful to Thierry Adatte (Institute of Earth Sciences) and Stéphanie Grand (Institute of Earth Surface Dynamics) for their technical and scientific supports. Finally, we thank the anonymous Reviewers for their useful comments.

Funding

This research was funded by the Ministero dell'Istruzione, dell'Università e della Ricerca through the PRIN 2010-2011 project (grant number 2010AYKTAB006; project leader C. Baroni), the project of strategic interest NEXTDATA (PNR National Research Program 2011-2013; project leader A. Provenzale CNR-ISAC). This work has besides benefited from the framework of the COMP-HUB Initiative (unipr), funded by the 'Departments of Excellence' program of the Italian Ministry for Education, University and Research (MIUR, 2018-2022).

References

Albrecht R, Sebag D and Verrecchia EP (2015) Organic matter decomposition: bridging the gap between Rock–Eval pyrolysis and chemical characterization (CPMAS 13C NMR). Biogeochemistry 122, 101–111.

Avery BW and Bascomb C L (Eds.) (1982) Soil survey laboratory methods. Lawes agricultural trust.

Balesdent J, Girardin C and Mariotti A (1993) Site-Related^(13) C of Tree Leaves and Soil Organic Matter in a Temperate Forest. Ecology, 74(6), 1713-1721.

Bascomb CL (1968) Distribution of pyrophosphate-extractable iron and organic carbon in soils of various groups. European Journal of Soil Science, 19(2), 251-268.

Beckage B, Osborne B, Gavin DG et al. (2008) A rapid upward shift of a forest ecotone during 40 years of warming in the Green Mountains of Vermont. Proceedings of the National Academy of Sciences, 105, 4197–4202.

Behar F, Beaumont V and De B. Penteado HL (2001) Rock-Eval 6 technology: performances and developments. Oil and Gas Science and Technology 56 (2), 111–134.

Briffa K and Jones P (1990) Basic chronology statistics and assessment. In Cook, ER and Kairiukstis, LA, editors, Methods of dendrochronology: applications in the environmental sciences, Dordrecht: Kluwer, 137-152.

Bollati I, Masseroli A, Mortara G et al. (2019) Alpine gullies system evolution: erosion drivers and control factors. Two examples from the western Italian Alps. Geomorphology 327, 248–263

612 Burga CA (1991) Vegetation history and palaeoclimatology of the Middle Holocene: Pollen analysis of
613 alpine peat bog sediments, covered formerly by the Rutor Glacier, 2510 m (Aosta Valley, Italy). Global
614 Ecology and Biogeography Letters, 1, 43–150.
615 Butler DR, Malanson GP, Bekker MF et al. (2003) Lithologic, structural, and geomorphic controls on ribbon
616 forest patterns in a glaciated mountain environment. Geomorphology, 55, 203–217
617 Butler DR, Malanson GP, Resler LM et al. (2009) Geomorphic patterns and processes at alpine treeline. In
618 The changing alpine treeline, vol. 12, ed. D. Butler, G. Malanson, S. Walsh, S. Fagre, 63–84.
619 Amsterdam: Elsevier.
620 Büntgen U, Esper J, Frank DC, Nicolussi K, and Schmidhalter, M (2005). A 1052-year tree-ring proxy for
621 alpine summer temperatures. Clim Dynam 25:141–153. doi:10.1007/s00382-005-0028-1
622 Büntgen U, Frank D, Wilson ROB et al. (2008) Testing for tree-ring divergence in the European Alps.
623 Global Change Biology, 14(10), 2443-2453.
624 Büntgen U, Tegel W, Nicolussi K et al. (2011) 2500 years of European climate variability and human
625 susceptibility. Science 331:578–582
626 Chersich S, Rejšek K, Vranová V et al. (2015) Climate change impacts on the Alpine ecosystem: an
627 overview with focus on the soil. Journal of Forest Science, 61(11), 496-514.
628 Coppola A, Leonelli G, Salvatore MC et al. (2012) Weakening climatic signal since mid-20th century in
629 European larch tree-ring chronologies at different altitudes from the Adamello-Presanella Massif
630 (Italian Alps). Quaternary research, 77(3), 344-354.
631 Coppola A, Leonelli G, Salvatore MC et al. (2013) Tree-ring-based summer mean temperature variations in
632 the Adamello-Presanella Group. Clim Past 9:211–221
633 Corona C, Guiot J, Edouard JL et al. (2010) Millennium-long summer temperature variations in the
634 European Alps as reconstructed from tree rings. Clim Past 6:379–400
635 Cremaschi M and Rodolfi G (1991) Il suolo - Pedologia nelle scienze della Terra e nella valutazione del
636 territorio. La Nuova Italia Scientifica, Roma.
637 D'Arrigo, R.D., Wilson, R., Liepert, B., Cherubini, P., 2008. On the "Divergence Problem" in Northern
638 Forests: A review of the tree-ring evidence and possible causes. Glob. Planet. Change 60, 289–305.
639 https://doi.org/10.1016/j.gloplacha.2007.03.004
640 D'Amico ME, Calabrese F and Previtali F (2009) Suoli di alta quota ed ecologia del Parco Naturale del Mont
641 Avic (Valle d'Aosta). Studi Trentini di Scienze Naturali, 85, 23-37.
642 D'Amico ME, Catoni M, Terribile F et al. (2016) Contrasting environmental memories in relict soils on
643 different parent rocks in the south-western Italian Alps. Quaternary International, 418, 61-74.
644 D'Amico ME, Freppaz M, Leonelli G et al. (2015) Early stages of soil development on serpentinite: the
645 proglacial area of the Verra Grande Glacier, Western Italian Alps. Journal of Soils and Sediments,
646 15(6), 1292-1310.

D'Amico ME, Pintaldi E, Catoni M et al. (2019) Pleistocene periglacial imprinting on polygenetic soils and paleosols in the SW Italian Alps. Catena, 174, 269-284.

Dal Piaz GV, Gianotti F, Monopoli B et al. (2010) Note illustrative della Carta Geologica d'Italia alla scala 1: 50.000, Foglio 091 Chatillon. Servizio Geologico d'Italia, Foglio, 91, 5-152.

Dawes MA, Schleppi P, Hättenschwiler S et al. (2017) Soil warming opens the nitrogen cycle at the alpine treeline. Global change biology, 23(1), 421-434.

Do Nascimento NR, Fritsch E, Bueno GT et al. (2008) Podzolization as a deferralitization process: dynamics and chemistry of ground and surface waters in an Acrisol–Podzol sequence of the upper Amazon Basin. European Journal of Soil Science, 59(5), 911-924.

Egli M and Poulenard J (2016) Soils of mountainous landscapes. International Encyclopedia of Geography: People, the Earth, Environment and Technology: People, the Earth, Environment and Technology, 1-10.

Egli M, Fitze P and Mirabella A (2001) Weathering and evolution of soils formed on granitic, glacial deposits: results from chronosequences of Swiss alpine environments. Catena, 45(1), 19-47.

Egli M, Merkli C, Sartori G et al. (2008) Weathering, mineralogical evolution and soil organic matter along a Holocene soil toposequence developed on carbonate-rich materials. Geomorphology, 97(3-4), 675-696.

Egli M, Mirabella A, Sartori G et al. (2006) Effect of north and south exposure on weathering rates and clay mineral formation in Alpine soils. Catena, 67(3), 155-174.

Egli M, Sartori G, Mirabella A et al. (2009) Effect of north and south exposure on organic matter in high Alpine soils. Geoderma, 149(1-2), 124-136.

Egli M, Sartori G, Mirabella A. et al. (2010) The effects of exposure and climate on the weathering of late Pleistocene and Holocene Alpine soils. Geomorphology, 114(3), 466-482.

Freppaz M and Williams MW (2015) Mountain soils and climate change. In: Romeo, R; Vita, A; Manuelli, S; Zanini, E; Freppaz, Michele; Stanchi, Silvia. Understanding Mountain Soils: A Contribution from mountain areas to the International Year of Soils 2015. Rome: FAO, 106-108.

Gale SJ and Hoare PG (1991) Quaternary Sediments: Petrographic Methods for the Study of Unlithified Rocks Belhaven, London, p. 323

Gehrig-Fasel J, Guisan A and Zimmermann NE (2007) Treeline shifs in the Swiss Alps: Climate change or land abandonment? Journal of Vegetation Science, 18, 571–582.

Gehrig-Fasel J, Guisan A and Zimmermann NE (2008) Evaluating thermal treeline indicators based on air and soil temperature using an air-to-soil temperature transfer model. ecological modelling, 213(3-4), 345-355.

Gerschlauer F, Saiz G, Schellenberger Costa, D et al. (2019) Stable carbon and nitrogen isotopic composition of leaves, litter, and soils of various ecosystems along an elevational and land-use gradient at Mount Kilimanjaro, Tanzania. Biogeosciences, 16(2), 409-424.

Hagedorn F, Mulder J and Jandl R (2010) Mountain soils under a changing climate and land-use. Biogeochemistry, 97(1), 1-5.

683 Harris I, Jones PD, Osborn TJ et al. (2014) Updated high-resolution grids of monthly climatic observations –
684 the CRU TS3.10 Dataset. Int. J. Climatol., 34: 623–642. (doi: 10.1002/joc.3711).
685 Holling CS (1973) Resilience and stability of ecological systems. Annual review of ecology and systematics,
686 4(1), 1-23.
687 Holtmeier FK and Broll G (2005) Sensitivity and response of northern hemisphere altitudinal and polar
688 treelines to environmental change at landscape and local scales. Global ecology and Biogeography,
689 14(5), 395-410.
690 Holtmeier FK and Broll GE (2007) Treeline advance-driving processes and adverse factors. Landscape
691 online, 1, 1-33.
692 Holtmeier FK and Broll G (2018) Soils at the Altitudinal and Northern Treeline: European Alps, Northern
693 Europe, Rocky Mountains-A Review. Insights of Forest Research, 2(1).
694 Hughes MK (2002) Dendrochronology in climatology–the state of the art. Dendrochronologia, 20(1-2), 95-
695 116.
696 Hughes NM, Johnson DM, Akhalkatsi M et al. (2009) Characterizing Betula litwinowii seedling microsites
697 at the alpine–treeline ecotone, Central Greater Caucasus Mountains, Georgia. Arctic, Antarctic and
698 Alpine Research, 41, 112–118.
699 IUSS Working Group WRB (2015) World Reference Base for Soil Resources 2014, update 2015
700 International soil classification system for naming soils and creating legends for soil maps. World Soil
701 Resources Reports No. 106. FAO, Rome.
702 Jahn R, Blume HP, Asio VB et al. (2006) Guidelines for soil description. FAO.
703 Jenny H (1941) Factors of soil formation: a system of quantitative pedology. McGraw-Hill book company
704 inc., New York.
705 Kjeldahl J (1883) Neue Methode zur Bestimmung des Stickstoffs in organischen Körpern. J. Anal. Chem.
706 22, 366–382
707 Klasner FL and Fagre DB (2002) A half century of change in alpine treeline patterns at Glacier National
708 Park, Montana, USA. Arctic, Antarctic, and Alpine Research, 34, 49–56.
709 Körner C (1999) Alpine Plant Life. Springer, Berlin.
710 Körner C and Paulsen J (2004) A world-wide study of high altitude treeline temperatures. Journal of
711 biogeography, 31(5), 713-732.
712 Kullman L (2001) 20th century climate warming and tree-limit rise in the southern Scandes of Sweden.
713 Ambio, 30, 72–80.
714 Kullman L and Öberg L (2009) Post-Little Ice Age tree line rise and climate warming in the Swedish
715 Scandes: A landscape ecological perspective. Journal of Ecology, 97, 415–429.
716 Lafargue E, Marquis F and Pillot D (1998) Rock-Eval 6 applications in hydrocarbon exploration, production,
717 and soil contamination studies. Oil and Gas Science and Technology 53 (4), 421–437.
718 Lamb HH (1995) “The little ice age”, Climate, history and the modern world, London, Routledge, 464 pp.

719 Legros JP (1992) Soils of Alpine mountains. In Developments in Earth Surface Processes (Vol. 2, pp. 155-
720 181). Elsevier.
721 Lehmann J and Kleber M (2015) The contentious nature of soil organic matter. Nature, 528(7580), 60.
722 Leonelli G, Masseroli A and Pelfini M (2016) The influence of topographic variables on treeline trees under
723 different environmental conditions. Physical Geography 37(1), 56-72.
724 Leonelli G, Pelfini M, Battipaglia G et al. (2009) Site-aspect influence on climate sensitivity over time of a
725 high-altitude Pinus cembra tree-ring network. Climatic Change 96, 185–201. doi:10.1007/s10584-009-
726 9574-6.
727 Leonelli G, Pelfini M, Morra di Cella U et al. (2011) Climate warming and the recent treeline shift in the
728 European Alps: the role of geomorphological factors in high–altitudes sites. Ambio, 40, 264–273.
729 Macias-Fauria M and Johnson EA (2013) Warming-induced upslope advance of subalpine forest is severely
730 limited by geomorphic processes. Proceedings of the National Academy of Sciences, 110(20), 8117-
731 8122.
732 Malanson GP, Resler LM, Butler DR et al. (2019) Mountain plant communities: uncertain sentinels?
733 Progress in Physical Geography 43 (4):521–543
734 Martinelli LA, Piccolo MDC, Townsend AR et al. (1999) Nitrogen stable isotopic composition of leaves and
735 soil: tropical versus temperate forests. Biogeochemistry, 46(1-3), 45-65.
736 Masseroli A, Bollati IM, Proverbio SS et al. (2020) Soils as a useful tool for reconstructing geomorphic
737 dynamics in high mountain environments: The case of the Buscagna stream hydrographic basin
738 (Lepontine Alps). Geomorphology, 107442.
739 Masseroli A, Leonelli G, Bollati I et al. (2016) The Influence of Geomorphological Processes on the Treeline
740 Position in Upper Valtellina (Central Italian Alps). Geogr. Fis. Dinam. Quat. 39 (2), 171-182, DOI
741 10.4461/ GFDQ 2016.39.16.
742 Matteodo M, Grand S, Sebag D et al. (2018) Decoupling of topsoil and subsoil controls on organic matter
743 dynamics in the Swiss Alps. Geoderma, 330, 41-51.
744 Mazepa VS (2005) Stand density in the last millennium at the upper tree-line ecotone in the Polar Ural
745 Mountains. Canadian Journal of Forest Research, 35, 2082–2091
746 Melvin, T.M., Briffa, K.R., 2008. A ‘‘signal-free’’ approach to dendroclimatic standardization.
747 Dendrochronologia 26 (2008) 71–86. doi:10.1016/j.dendro.2007.12.001.
748 Melvin, T.M., Briffa, K.R., 2014. CRUST: Software for the implementation of Regional Chronology
749 Standardisation: Part 1. Signal-Free RCS. Dendrochronologia 32, 7–20.
750 https://doi.org/10.1016/j.dendro.2013.06.002
751 Menzel A and Fabian P (1999) Growing season extended in Europe. Nature 397, 659.
752 Menzel A, Sparks TH, Estrella N et al. (2006) European phonological response to climate change matches
753 the warming pattern. Global Change Biology 12 (10), 1969–1976.

754 Mercalli L, Cat Berro D and Montuschi S (2003) Atlante climatico della Valle d'Aosta, 416 pp. Turin:
755 Società Meteorologica Subalpina.
756 Merkli C, Sartori G, Mirabella A et al. (2009) The soils in the Brenta region: chemical and mineralogical
757 characteristics and their relation to landscape evolution. Studi Trentini di Scienze Naturali, 85, 7-22.
758 Ministero delle Risorse Agricole Alimentari e Forestali (1994). Metodi ufficiali di analisi chimica del suolo,
759 con commenti ed interpretazioni. ISMEA, Roma, 207 pp.
760 Müller M, Schickhoff U, Scholten T et al. (2016) How do soil properties affect alpine treelines? General
761 principles in a global perspective and novel findings from Rolwaling Himal, Nepal. Progress in Physical
762 Geography, 40(1), 135-160.
763 Nicolussi K, Kaufmann M, Melvin TM et al. (2009) A 9111 year long conifer tree-ring chronology for the
764 European Alps: a base for environmental and climatic investigations. The Holocene, 19(6), 909-920.
765 Nicolussi K, Kauffman M, Patzelt G et al. (2005) Holocene tree-line variability in the Kauner valley, central
766 Eastern Alps, indicated by dendrochronological analysis of living trees and subfossil logs. Veg Hist
767 Archaeobot 14:221–234.
768 Peel MC, Finlayson BL and McMahon TA (2007) Updated world map of the Köppen-Geiger climate
769 classification. Hydrology and Earth System Sciences, 11 (5), 1633–1644. doi: 10.5194/hess-11-1633-
770 2007.
771 Pelfini M, Leonelli G, Trombino L et al. (2014) New data on glacier fluctuations during the climatic
772 transition at similar to 4,000 cal. year BP from a buried log in the Forni Glacier forefield (Italian Alps)
773 Rendiconti Lincei-Scienze Fisiche e Naturali, 25 (4), 427-437.
774 Phillips JD and Marion DA (2004) Pedological memory in forest soil development. Forest Ecology and
775 Management, 188(1-3), 363-380.
776 Scapozza C, Lambiel C, Reynard E et al. (2010) Radiocarbon dating of fossil wood remains buried by the
777 Piancabella rock glacier, Blenio Valley (Ticino, Southern Swiss Alps): implications for rock glacier,
778 treeline and climate history. Permafrost and Periglacial Processes, 21, 90–96.
779 Schatz AK, Zech M, Buggle B et al. (2011) The late Quaternary loess record of Tokaj, Hungary:
780 reconstructing palaeoenvironment, vegetation and climate using stable C and N isotopes and
781 biomarkers. Quaternary International, 240(1-2), 52-61.
782 Schomburg A, Sebag D, Turberg P et al. (2019) Composition and superposition of alluvial deposits drive
783 macro-biological soil engineering and organic matter dynamics in floodplains. Geoderma, 355, 113899.
784 Schomburg A, Verrecchia EP, Guenat C et al. (2018) Rock-Eval pyrolysis discriminates soil macro-
785 aggregates formed by plants and earthworms. Soil Biology and Biochemistry, 117, 117-124.
786 Sebag D, Verrecchia EP, Cécillon L et al. (2016) Dynamics of soil organic matter based on new Rock-Eval
787 indices. Geoderma, 284, 185-203.
788 Sparks TH and Menzel A (2002) Observed changes in the seasons: an overview. International Journal of
789 Climatology 22, 1715–1725.

790 Stevenson BA, Kelly EF, McDonald EV et al. (2005) The stable carbon isotope composition of soil organic
791 carbon and pedogenic carbonates along a bioclimatic gradient in the Palouse region, Washington State,
792 USA. Geoderma, 124(1-2), 37-47.
793 Sullivan PF, Ellison SB, McNown RW et al. (2015) Evidence of soil nutrient availability as the proximate
794 constraint on growth of treeline trees in northwest Alaska. Ecology, 96(3), 716-727.
795 Virtanen R, Luoto M, Rämä T et al. (2010) Recent vegetation changes at the high-latitude tree line ecotone
796 are controlled by geomorphological disturbance, productivity and diversity. Global Ecology and
797 Biogeography, 19, 810–821
798 Vittoz P, Rulence B, Largey T et al. (2008) Effects of climate and land-use change on the establishment and
799 growth of Cembran pine (*Pinus cembra* L.) over the altitudinal treeline ecotone in the Central Swiss
800 Alps. Arctic, Antarctic, and Alpine Research, 40, 225–232.
801 Walkley A and Black IA (1934) An examination of the Degtjareff method for determining soil organic
802 matter, and proposed modification of the chromic acid titration method. Soil Sci, 37(1), 29-38.
803 Walther GR, Post E, Convey P et al. (2002) Ecological responses to recent climate change. Nature 416, 389–
804 395.
805 Wang T, Zhang QB and Ma K (2006) Treeline dynamics in relation to climatic variability in the central
806 Tianshan Mountains, northwestern China. Global Ecology and Biogeography, 15(4), 406-415.
807 Waroszewski J, Kalinski K, Malkiewicz M et al. (2013) Pleistocene–Holocene cover-beds on granite regolith
808 as parent material for Podzols—an example from the Sudeten Mountains. Catena, 104, 161-173.
809 Zanelli R, Egli M, Mirabella A et al. (2007) Vegetation effects on pedogenetic forms of Fe, Al and Si and on
810 clay minerals in soils in southern Switzerland and northern Italy. Geoderma, 141(1-2), 119-129.
811 Zanini E, Freppaz M, Stanchi S et al. (2015) Soil variability in mountain areas. In: Romeo, R; Vita, A;
812 Manuelli, S; Zanini, E; Freppaz, Michele; Stanchi, Silvia. Understanding Mountain Soils: A
813 Contribution from mountain areas to the International Year of Soils 2015. Rome: FAO, 60-62.
814 Zech M, Zech R and Glaser B (2007) A 240,000-year stable carbon and nitrogen isotope record from a loess-
815 like palaeosol sequence in the Tumara Valley, Northeast Siberia. Chemical Geology, 242(3-4), 307-318.
816
817
818 **Figures**

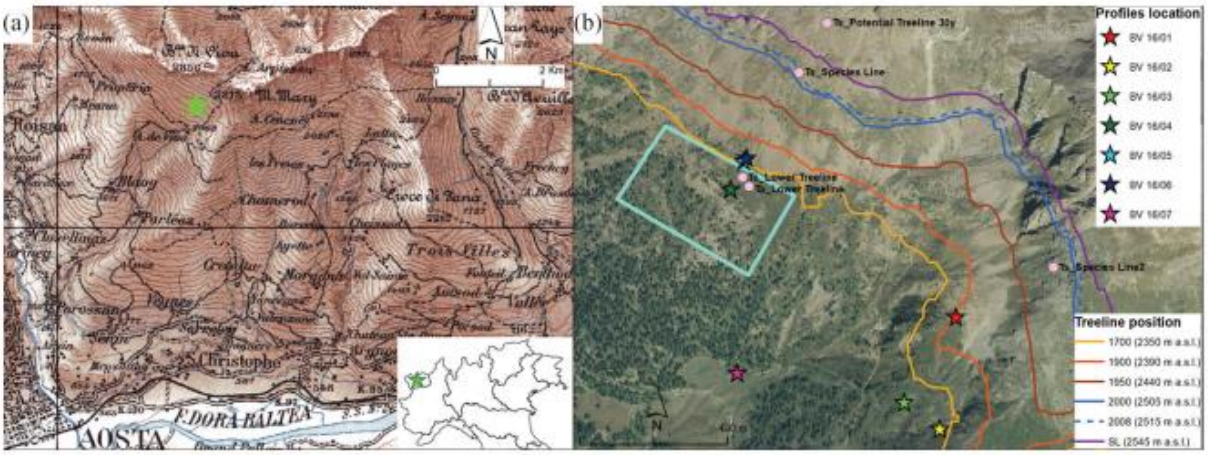

Figure 1. (a) Study area and Becca di Viou site location (green star; topographic map from National Geoportal http://www.pcn.minambiente.it/GN/); (b) Locations on the Becca di Viou slope of the soil profiles (stars), of the dendrochronological sampling area (light blue rectangle) and of the dataloggers (pink dots). In the figure the treeline positions over 1700–2000 for 50-year time periods, the treeline position in in 2008 and the species line (SL) are also depicted (from Leonelli et al., 2011).

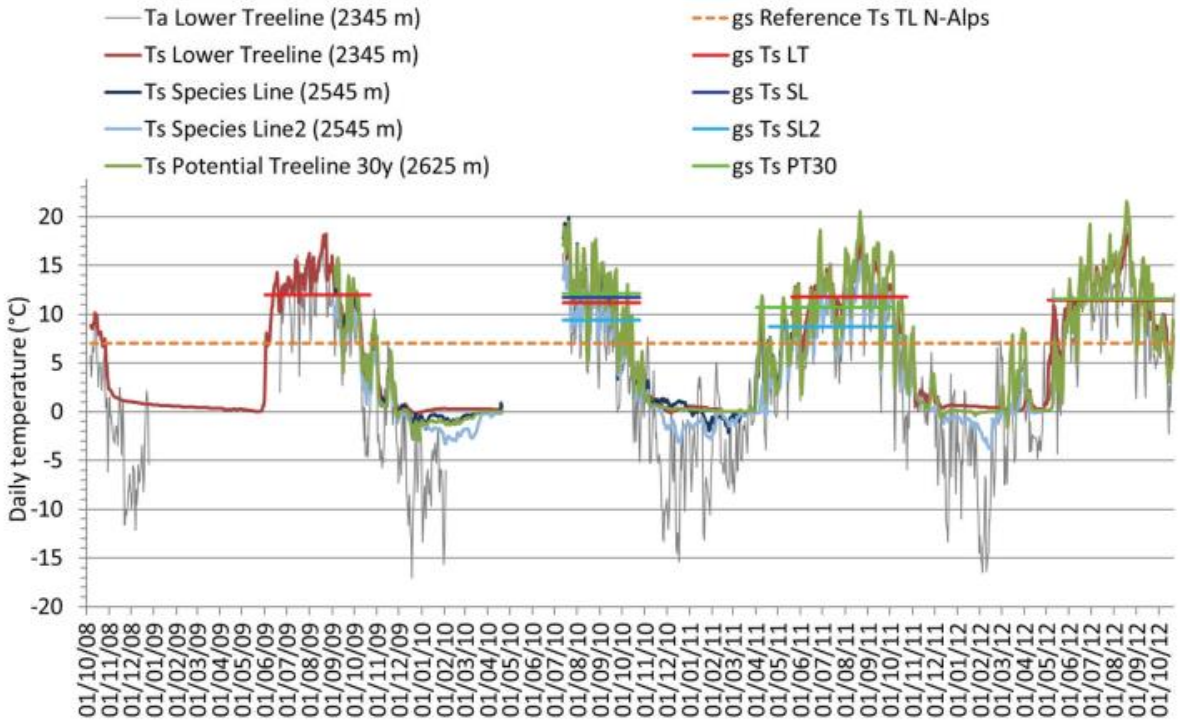

Figure 2. Average daily air (Ta) and soil (Ts) temperatures measured at different positions in the treeline belt between October 2008 and October 2012: Lower Treeline, LT; Species Line, SL; Potential Treeline 30 years, PT30 (the latter is defined by the altitude with more than 100 days per year with an air temperature > 5 °C over the 30-yr period 1975–2004; Leonelli et al., 2011); in brackets the altitude of the dataloggers (m a.s.l.) The horizontal lines depict the average soil temperature of the growing season (gs), defined by the first day with soil temperature > 3.2 °C (beginning) up to the first day with a soil temperature < 3.2 °C (end of the growing season; Körner and Paulsen, 2004). The dashed horizontal line depicts the reference soil temperature for the treelines in the Swiss Alps, i.e. 7 °C (Gehrig-Fasel et al., 2008).

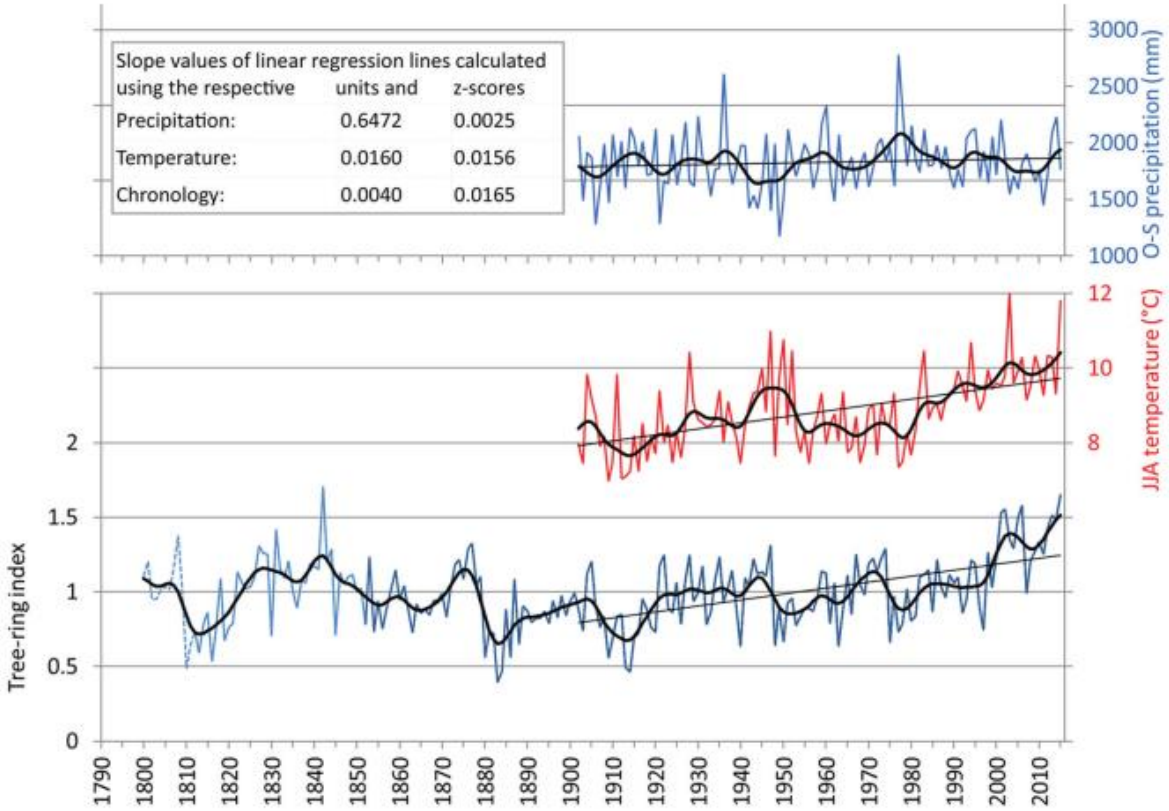

Figure 3. At the bottom, the signal-free chronology of the Becca di Viou site over the period 1800-2015 (dark blue line = EPS >0.85 since 1852; light blue = EPS >0.71 since 1812; dashed light blue for the previous period since AD 1800). The graph also depicts the June-to-August mean temperature (JJA; in red) and the October-to-September total precipitations (i.e. a 12-month water year; in blue) over the period 1902-2015.
All the series are smoothed with a 20-yr Gaussian low-pass filter with standard deviation set to 4 yr (black lines) and a fitting regression line whose slope value referred to the respective units and to z-scores is reported in the table in the top-left corner.

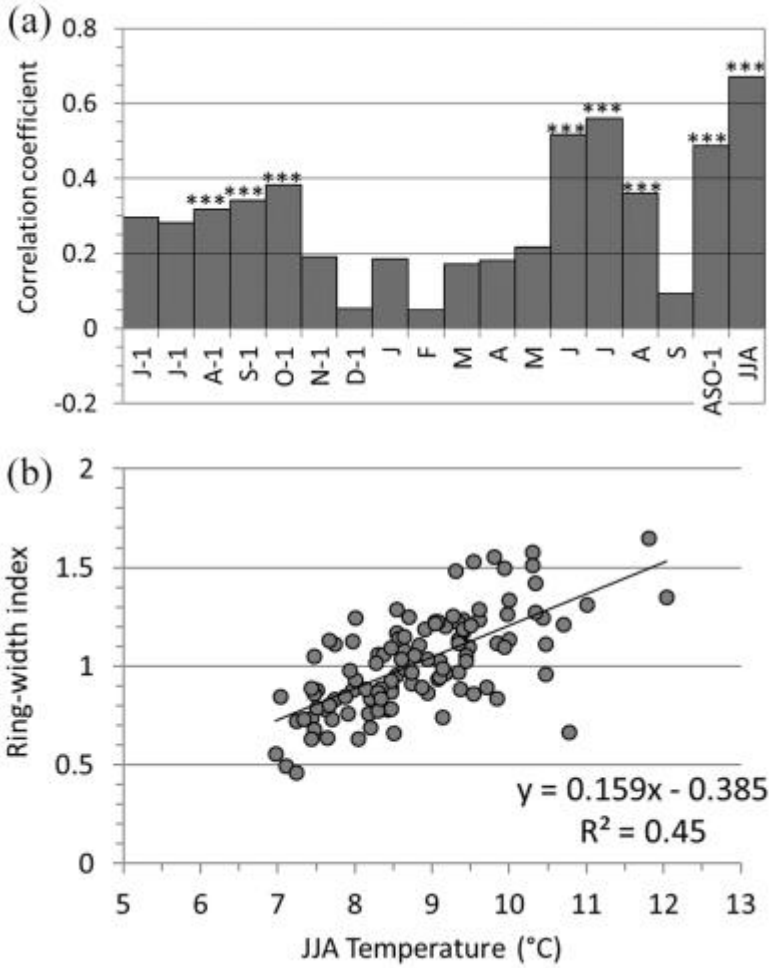

Figure 4. (a) Correlation coefficient calculated over the period 1902-2015 between the signal-free chronology and the monthly temperature variables from June of the previous year to September. *** = $p < 0.001$. (b) Linear regression of ring-width indices of the signal-free chronology on summer (JJA) temperatures; the coefficient of determination and the regression equation are also reported.

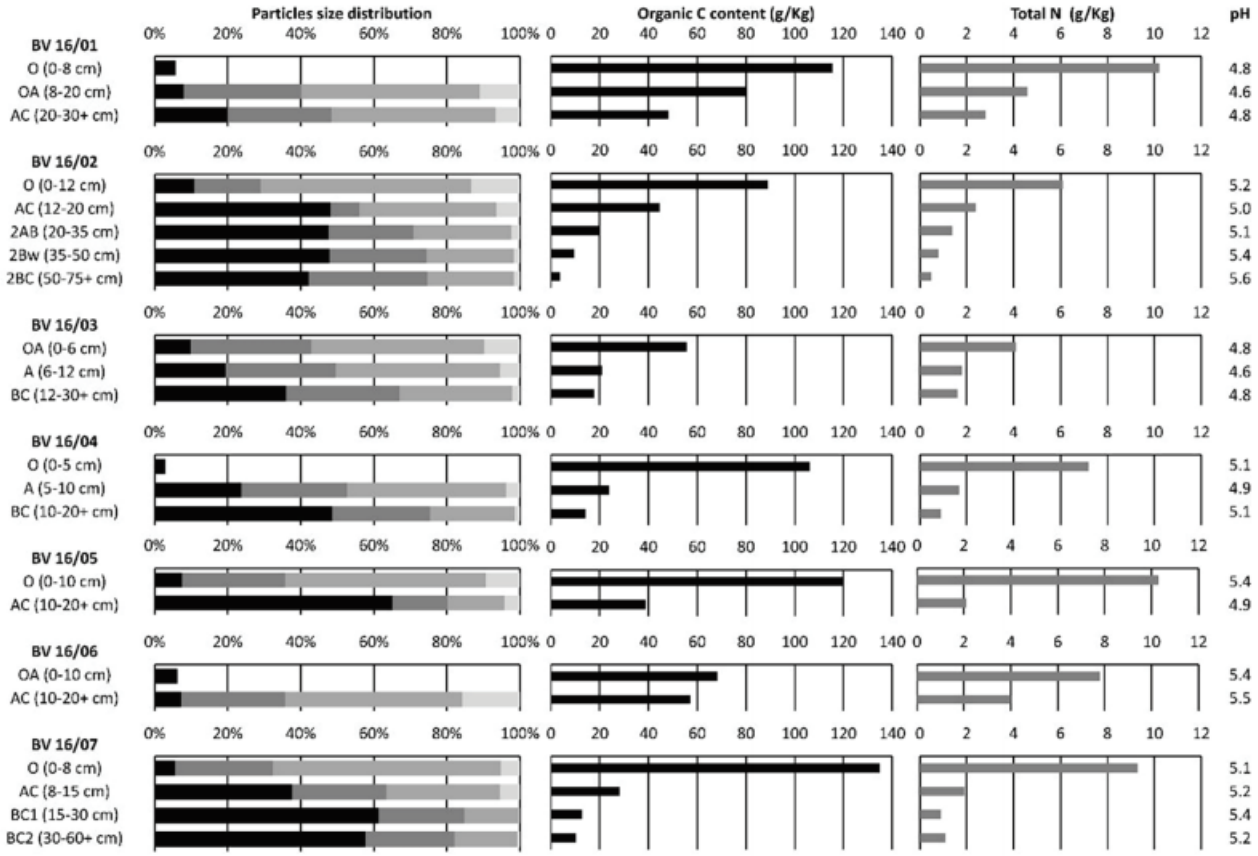

Figure 5. Particle size distributions, organic C contents (C org.), total N contents, and pH(H_2O) values in the studied profiles. In plots of particle size distributions, the gravel, sand, silt, and clay contents are depicted in black, dark grey, grey and light grey, respectively.

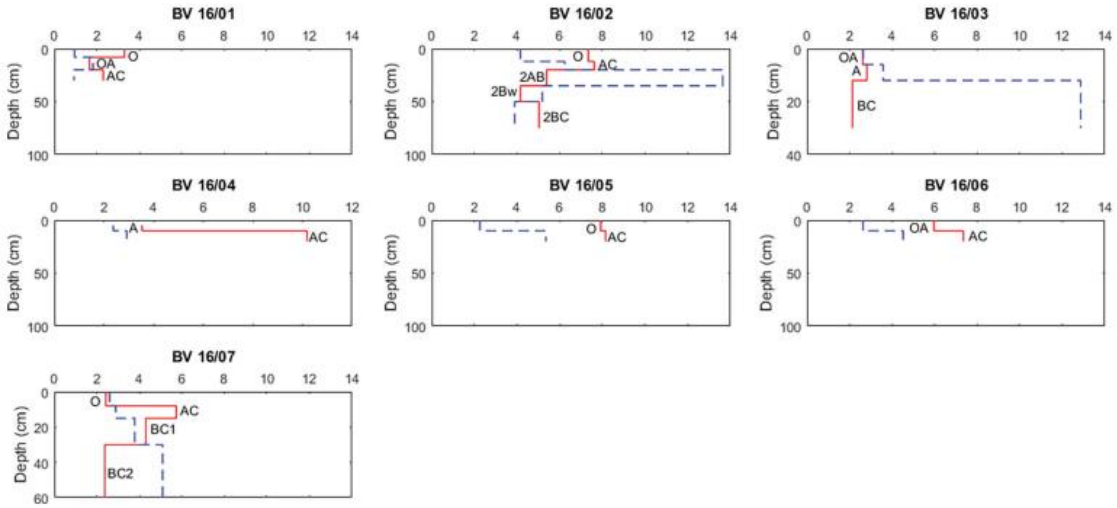

Figure 6. Variations in the studied profiles of crystalline iron oxides (Fe_{cry} = Fe_d-Fe_o, red line; g/Kg) and ammonium oxalate extractable Fe (Fe_o, as a measurement of the "activity" of the iron oxides, blue dotted line; g/Kg). Horizon names are displayed close to the Fe_{cry} curves.

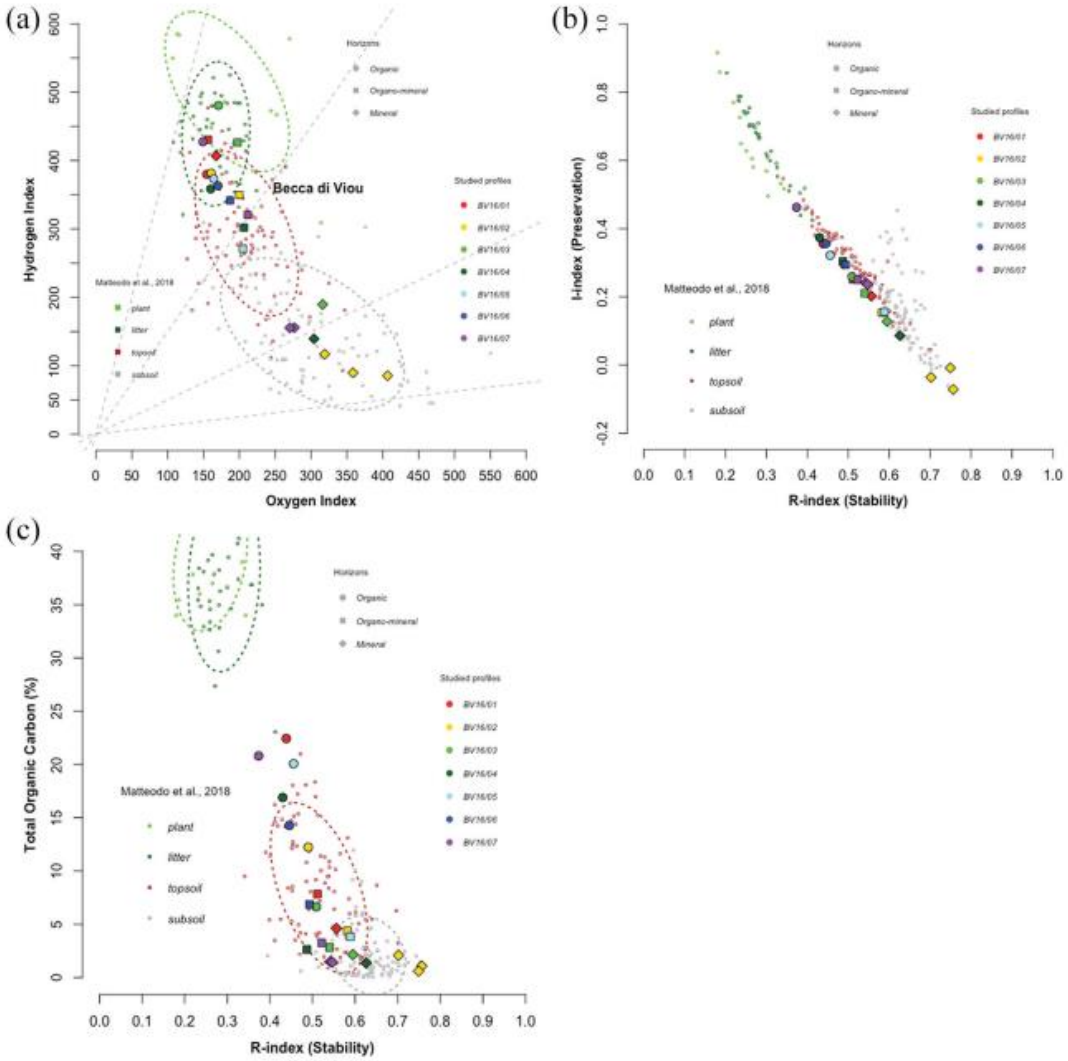

Figure 7. (a) HI (mg HC/g TOC)/OI (mg CO_2/g TOC) diagram; (b) I-index/R-index of the studied horizons; (c) Total Organic Carbon content % (TOC)/R-index of the studied horizon. Shapes refer to the horizon type (organic, organo-mineral, or mineral) and colors to the profile number. Small colored dots, plotted in the background for comparison, are from Matteodo et al. (2018)'s dataset composed of 46 soil profiles selected across various eco-units in the Swiss Alps.

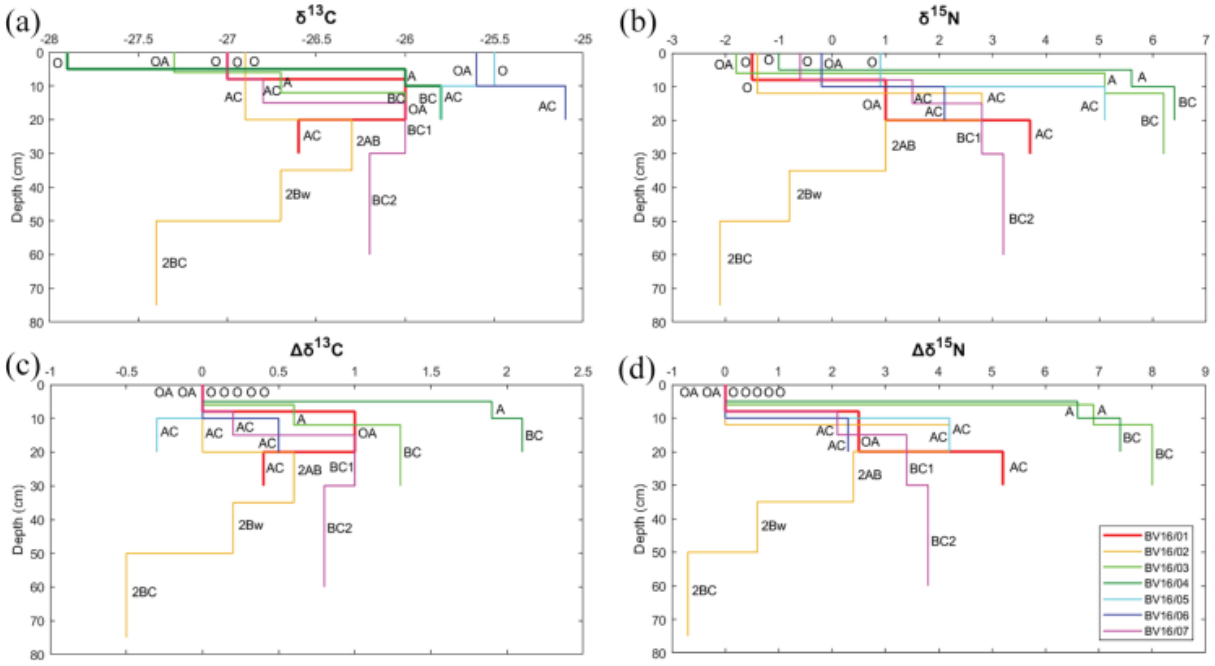

Figure 8. (a) $\delta^{13}C$ (‰) values of studied profiles; (b) $\delta^{15}N$ (‰) values of studied profiles; (c) $\Delta\delta^{13}C$ (‰) content of studied profiles, isotopic enrichment with reference to the first horizon; (d)$\Delta\delta^{15}N$ (‰) content of studied profiles, isotopic enrichment with reference to the first horizon.

877 **Tables**

878

Table 1. Site descriptions of the investigated soil profiles. The profile exposure is the same as the slope exposure.

Profile	Elevation (m a.s.l.)	Slope (°)	Slope exposure	Parent material	Landform	Vegetation
BV16/01	2400	10	N	Slope deposits composed of Gneiss and Schists	Upper slope	Treeline ecotone, open stands of *Larix decidua* and grassland
BV16/02	2340	20	NW	Slope deposits composed of Gneiss and Schists	Upper slope	Treeline ecotone, open stands of *Larix decidua* and grassland
BV16/03	2300	30	W-NW	Slope deposits composed of Gneiss and Schists	Upper slope	Treeline ecotone, open stands of *Larix decidua* and grassland
BV16/04	2325	15	W-SW	Slope deposits composed of Gneiss and Schists	Upper slope	Treeline ecotone, open stands of *Larix decidua*
BV16/05	2365	25	S-SW	Slope deposits composed of Gneiss and Schists	Upper slope	Treeline ecotone, open stands of *Larix decidua*
BV16/06	2370	25	S-SW	Slope deposits composed of Gneiss and Schists	Upper slope	Treeline ecotone, open stands of *Larix decidua*
BV16/07	2110	20	S-SW	Slope deposits composed of Gneiss and Schists	Middle slope	*Larix decidua* woodland

879

880

881

882

Table 2. Dithionite (d)- and oxalate (o)- extractable contents of Fe and Al. Crystalline iron oxides ($Fe_{cry} = Fe_d - Fe_o$), activity iron index (Fe_o/Fe_d) and podzolization index ($Al_o + 1/2Fe_o$).

Profile	Horizon	Depth (cm)	Al_d (g/Kg)	Fe_d (g/Kg)	Al_o (g/Kg)	Fe_o (g/Kg)	Fe_o/Fe_d	$Fe_{cry} = Fe_d - Fe_o$ (g/Kg)	$Al_o + 1/2Fe_o$ (%)
BV16/01	O	0–8	1.23	4.25	1.02	0.95	0.22	3.30	0.15
	OA	8–20	1.41	3.47	2.70	1.82	0.52	1.65	0.36
	AC	20–30+	2.16	3.23	2.60	0.93	0.29	2.30	0.31
BV16/02	O	0–12	2.40	11.50	2.46	4.16	0.36	7.34	0.45
	AC	12–20	3.10	13.85	2.58	6.23	0.45	7.62	0.57
	2AB	20–35	5.82	19.03	6.01	13.64	0.72	5.39	1.28
	2Bw	35–50	5.73	9.34	5.58	5.18	0.55	4.16	0.82
	2BC	50–75+	5.30	8.92	4.47	3.89	0.44	5.03	0.64
BV16/03	OA	0–6	1.84	5.26	1.43	2.64	0.50	2.62	0.27
	A	6–12	1.35	6.39	2.29	3.58	0.56	2.80	0.41
	BC	12–30+	3.44	15.00	4.19	12.87	0.86	2.13	1.06
BV16/04	O	0–5	0.99	4.86	0.63	<0.90	n.d.	n.d.	n.d.
	A	5–10	1.74	5.92	2.06	2.38	0.40	3.54	0.32
	AC	10–20+	3.41	13.11	2.23	2.92	0.22	10.19	0.37
BV16/05	O	0–10	3.36	10.18	1.56	2.26	0.22	7.91	0.27
	AC	10–20+	3.12	13.50	2.58	5.35	0.40	8.15	0.53
BV16/06	OA	0–10	2.22	8.60	1.12	2.63	0.31	5.97	0.24
	AC	10–20+	4.01	11.87	1.75	4.52	0.38	7.35	0.40
BV16/07	O	0–8	2.55	5.02	1.23	2.60	0.52	2.42	0.25
	AC	8–15	2.12	8.63	1.22	2.89	0.33	5.74	0.27
	BC1	15–30	3.74	8.08	3.17	3.78	0.47	4.30	0.51
	BC2	30–60+	3.79	7.46	4.32	5.09	0.68	2.37	0.69

<: low values approximate to the minor concentration detectable; n.d.: no data.

883

884